Effect of fiber orientation in dynamic FTIR study on native cellulose

Barbara Hinterstoisser,[b] Margaretha Åkerholm,[a] Lennart Salmén[a],*

[a]STFI, Swedish Pulp and Paper Research Institute, Box 5604, SE-114 86 Stockholm, Sweden
[b]Institute of Chemistry, University of Agricultural Sciences, Muthgasse 18, A-1190 Vienna, Austria

Abstract

The properties of cellulose materials are highly dependent on the interactions between and within the cellulose chains mainly related to inter- and intramolecular hydrogen bonds. To investigate the deformation behavior of cellulose and its relation to molecular straining, cellulose sheets with different fiber orientations were studied by dynamic FTIR spectroscopy. The sheets were stretched sinusoidally at low strains while being irradiated with polarized infrared light. It is shown that the polarization direction determines the dynamic IR response to a higher extent than the fiber direction in the sample sheets. Different polarization modes give different dynamic signals, allowing conclusions to be drawn on the structural orientation of submolecular groups in the cellulose molecules. The bands in the spectra mainly affected by the deformation of the sheets were derived from skeletal vibrations that include the C–O–C bridge connecting adjacent rings and from the hydrogen bonds. The conclusion that these groups are the ones that are mainly deformed under load has thereby experimentally demonstrated the theoretical calculations from Tashiro and Kobayashi [Tashiro, K.; Kobayashi, M. *Polymer* **1991**, *32*, 1516–1526]. © 2001 Published by Elsevier Science Ltd.

1. Introduction

Cellulose is the dominant polymer in the biosphere. It is an optically anisotropic system being made up of poly-β(1 → 4)-β-D-glucose chains. On first sight, the molecular structure gives the impression of its being a very simple molecule, but in fact its structural characteristics have not yet been fully resolved.[2,3] The numerous strongly polar groups make cellulose molecules predestined for building up hydrogen bonds within the molecule and between the different molecules. In the gener- ally accepted structure of cellulose I, intramolecular hydrogen bonds of types 3-OH⋯O-5 and 2-OH⋯O-6 are present for both sides of the chain.[4] As a result of hydroxyl groups showing different polarities, cellulose has different crystalline structures, ranging from cellulose I (native cellulose) to cellulose IV. Moreover, cellulose I is itself composed of two different crystalline forms: cellulose Iα and Iβ.[5] From crystallographic studies, it has been concluded that the secondary structure of native cellulose is a ribbon-like conformation with approximately twofold helical structure.[3] Two chains, which take an almost fully extended conformation, are contained in the unit cell of cellulose I.

---

* Corresponding author. Tel.: + 46-8-6767340; fax: + 46-8-4115518.
 E-mail address: lennart.salmen@stfi.se (L. Salmén).

The cellulose molecule chain itself is not very stiff, but rather semiflexible. Calculations by Tashiro and Kobayashi,[1] based on the force constants proposed by Cael et al.,[6] have shown that the strain energy is distributed mainly to the deformation of the glucose rings ($\sim 30\%$), the bending of the ether linkages connecting the adjacent rings ($\sim 20\%$), and the 3-OH$\cdots$O-5 hydrogen bond ($\sim 20\%$). The Young's modulus of the cellulose chain is governed by strong intramolecular hydrogen bonds, mainly the 3-OH$\cdots$O-5 hydrogen bond. It is generally known and accepted that the hydrogen bonds play an important role in the conformational and mechanical properties of cellulosic materials.[2] However, several questions concerning the structure and dynamic behavior of native cellulose are still left unanswered.

Besides its complex crystalline structure, native cellulose also has a complex arrangement within the wood fiber wall. In the secondary wall, the cellulose chains are grouped into fibrils by hydrogen bonds. These fibrils are aligned in different directions in the different secondary wall layers. Such complexities in fibril alignment are what renders wood pulp fibers used in paper sheets into a much more complicated material compared to other materials, such as synthetic polymers.

Infrared spectroscopy, which is known to be sensitive to structural features, has had a long tradition in cellulose research. Since the very first use of infrared spectroscopy to elucidate molecular structures, much effort has been devoted to separating the overlapping bands deriving, for example, from hydrogen bonds.[1,4,7–12]

The development of a combination of dynamic mechanical analysis (DMA) and IR spectroscopy has brought new possibilities for assigning and interpreting spectra of polymer molecules, and subsequently for investigating intra- and intermolecular interactions.[13,14] An external perturbation, e.g., a small amplitude oscillatory strain, induces selectively time-dependent reorientations of electric dipole transition moments that are associated with the individual normal vibrational modes in the sample. The altered orientation distribution of dipole transition moments can be detected as a variation of the directionally sensitive IR absorbance of the system. By applying IR correlation analysis,[15] the obtained dynamic IR spectra can be transformed into a pair of so-called 2D IR correlation spectra to accentuate the differences among the reorientation rates. These spectra provide information about the interactions within and between the polymer chains. Dynamic 2D FTIR is capable of correlating the IR responses of each functional group in the polymer with either the applied mechanical strain or the IR responses of other functional groups. The technique was introduced to cellulose investigation by Hinterstoisser and Salmén.[16,17]

The work presented herein focuses on the inter- and intramolecular interactions within cellulose, the dynamic behavior of submolecular groups, and their relation to stresses in the sample sheet, as well as the effect of fiber orientation on the spectra obtained.

2. Materials and methods

Cellulose samples.—A spruce-dissolving pulp, provided by Borregaard, with a cellulose content of 98%, was used to make nonoriented and oriented sheets with a thickness of about 40 μm. The pulp was homogenized by pumping it several times through a slit (0.3–0.4 mm) in a laboratory homogenizer (Gaulin Corp.). The nonoriented sheets were made on a Finish sheet former with a grammage of 25 g/m². The oriented sheets with a grammage of 20 g/m² were made on a Formette Dynamique at a speed of rotation of 1600 rpm. The dichroic ratio of 1.43 for the 1160 cm^{-1} band, a skeletal vibration essentially in parallel with the backbone of cellulose, illustrates the orientation achieved for the sheets. The dichroic ratio is determined as the ratio between the absorption intensities at 0° and 90° polarization of the IR beam.

Dynamic FTIR experiments.—The dynamic FTIR experiments were performed on a Bio-Rad FTS 6000 FTIR spectrometer equipped with a Manning Polymer Modulator[18] mounted in the sample compartment. The interferometer worked in the step-scan mode, with a phase modulation frequency of 400 Hz

(the mirror oscillates around each step point with a frequency of 400 Hz). The effect of phase modulation is to emphasize the higher frequency information.
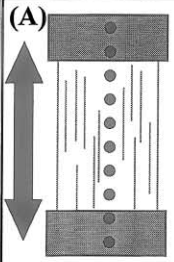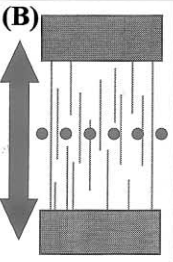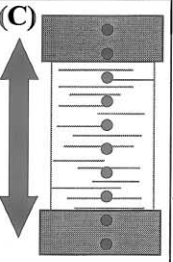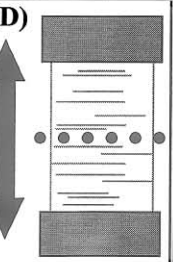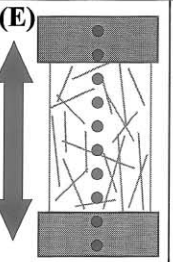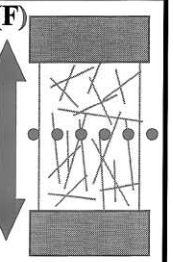
The infrared beam was polarized 0 and 90°, respectively, to the direction of the stretching motion. An additional optical filter was placed after the polarizer to reduce the spectral range (3950–700 cm^{-1}). Samples with a length of 35 mm and a width of 25 mm were cut out, mounted between the jaws of the Polymer Modulator, and prestretched to reduce buckling upon relaxation. The prestretching causes a change in thickness of the sheets, but the resulting spectral features can be regarded as being an order of magnitude smaller than the observed signals. During the subsequent repetitive stretching (sample modulation frequency: 16 Hz; stretching amplitude of less than 0.3% (~ 55 μm)), the infrared responses were recorded using a liquid-nitrogen-cooled MCT (mercury cadmium telluride) detector. Four scans with a resolution of 8 cm^{-1} were performed for each sample using asymmetric interferogram symmetry.

The stretcher operated at a known repeatable phase angle with respect to the interferometer steps. Two modulations occurred during the experiment: The low-frequency sample modulation and the high-frequency phase modulation of the mirror, as used in the digital signal processing. Two levels of demodulation were therefore required to extract the spectral response of the sample modulation from the detector signal. The interferograms thus obtained were Fourier transformed and a triangle apodization function was used. The obtained in-phase and out-of-phase spectra, are the result of the dynamic changes in the IR transmission spectrum due to the small oscillatory strain applied to the cellulose sheets. The spectra were normalized by division with the static transmission spectrum and then baseline corrected (one point baseline correction at a wavenumber of 2200 cm^{-1}). Six different kinds of experiments were performed (cf. Table 1).

For each experiment, several measurements were made with a small variation in the static stress. In order to make correct averages, the dynamic spectra had to be normalized. The spectral result from each measurement was divided into a phase spectrum and a magnitude spectrum. All magnitude spectra were then normalized to 1.0 at 1169 cm^{-1} (0° polarization) or 1165 cm^{-1} (90° polarization) and new in-phase and out-of-phase spectra were calculated from these. These normalized in-phase and out-of-phase spectra were then used for the mean dynamic spectra for each

Table 1
Orientation of the cellulose fibers and polarization modes relative to the stretching direction in the different experiments [a]

	(A)	(B)	(C)	(D)	(E)	(F)
Schematic drawing of the experiment / Fiber —— / Stretching direction						
Fiber orientation relative to stretching motion	parallel	parallel	perpendicular	perpendicular	none	none
Polarization relative to stretching motion	0° polarization	90° polarization	0° polarization	90° polarization	0° polarization	90° polarization

[a] A, fiber orientation parallel to stretching motion, polarization 0° to stretching motion; B, fiber orientation parallel to stretching motion, polarization 90° to stretching motion; C, fiber orientation perpendicular to stretching motion, polarization 0° to stretching motion; D, fiber orientation perpendicular to stretching motion, polarization 90° to stretching motion; E, no fiber orientation, polarization 0° to stretching motion; F, no fiber orientation, polarization 90° to stretching motion.
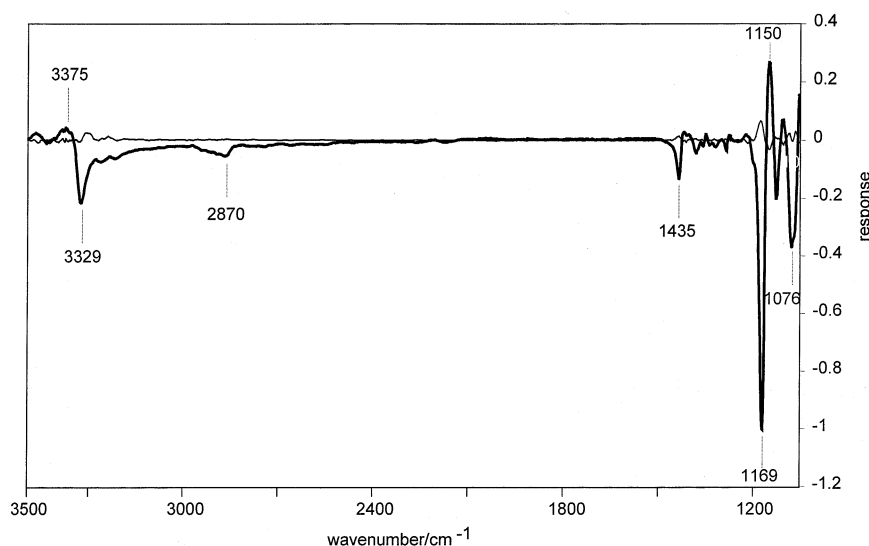
Fig. 1. In-phase (thick line) and out-of-phase (thin line) spectra of cellulose. The fibers of the cellulose sheet are oriented parallel to the stretching direction and the polarization plane of the incident beam is parallel (0°) to the strain direction. The most intense bands are marked.
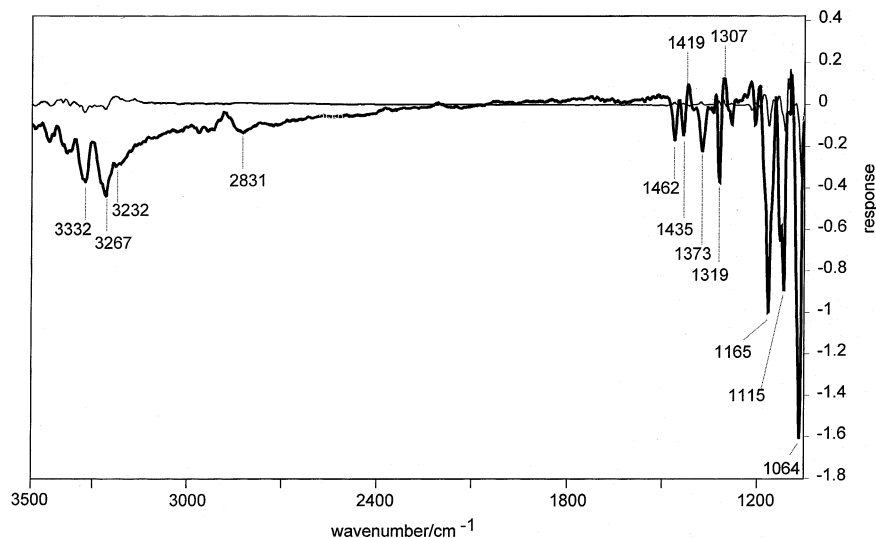

Fig. 2. In-phase (thick line) and out-of-phase (thin line) spectra of cellulose. The fibers are stretched parallel to their axis while the polarization plane of the incident beam is perpendicular (90°) to the stretching direction.

experiment. The spectra shown in the paper are all mean spectra.

The dynamic spectra, namely the mean in-phase and the mean out-of-phase, were used in a cross-correlation analysis according to Noda,[15] giving the synchronous and the asynchronous spectra. While the synchronous correlation intensities characterize the degree of coherence between the dynamic fluctuations of IR signals measured at two independent wavenumbers, the asynchronous correlation intensity characterizes the independent and

uncoordinated fluctuations of the IR signals. For the final discussion, only the synchronous plot was used here.

3. Results

Effect of polarization.—In Figs. 1 and 2, the in-phase and out-of-phase spectra of the oriented samples which were stretched parallel to the fiber direction are given for the cases of light polarized 0° (experiment A) and 90° (ex-

periment B) to the strain direction, respectively. The signal intensities of the out-of-phase spectra in both polarization directions were several times less than those of the in-phase spectra. This reflects the elastic response of the sample. In general, more peaks appeared in the in-phase spectra of the 90° polarization than at 0°, both in the OH-region and in the fingerprint region. The most intense peaks in the latter were found between 1200 and 1050 cm^{-1}.

At 0° polarization, the most intense peak was placed at 1169 cm^{-1}, and it was split with the responding positive peak at 1150 cm^{-1}. These are assigned as deriving from skeletal stretching vibrations including the C–O–C bridge stretching[19–21] which occur parallel to the molecular chain axis. Tashiro and Kobayashi[1] calculated a band at 1167 cm^{-1} for the skeletal vibration in general. At 90° polarization, a slightly different band position compared to the 0° polarization experiment can be observed for the mentioned C–O–C bridge stretching, being positioned at 1165 cm^{-1}. Further noticeable differences to the 0° polarization mode were that the peak was not split and neither was it the main peak. In this case, the 1064 cm^{-1} band in the C–O valence-vibration region was the most intense peak. At 0° polarization, on the other hand, the 1064 cm^{-1} seemed to appear as a shoulder of the 1076 cm^{-1} band.

For both directions of the electromagnetic field, a split peak at 1435 cm^{-1} (corresponding peak at 1419 cm^{-1}) was found, which might be a CH_2 scissors motion response according to the literature.[20] It should be noted that the 90° polarization experiment also had a peak at 1462 cm^{-1}, which could not be seen in the 0° polarization. This peak could, according to the calculations of Tashiro and Kobayashi,[1] have derived from CH_2 bending vibrations. On the other hand, in Raman measurements of ramie cellulose,[22] peaks appeared at 1456 and 1475 cm^{-1}, those being the most intense at 90° polarization of the incident beam. These have been assigned as HCH and HOC bending vibrations. The scissors motion involves a symmetric bending of the HCH angle. It seems plausible that the HCH bending is the Raman-active one and the HOC

bending is responsible for the observed infrared response.[19]

Between 1200 and 1500 cm^{-1}, several CH-deformation vibrations should be seen. Since the CH bonds are mainly oriented orthogonal to the ring and the fiber axis, more signals are expected to be found in the 90° polarization experiment, as can be observed in Fig. 2.

With regard to the OH-region, the dominating signal in the in-phase spectra for 0° polarization was at 3329 cm^{-1}. For the 90° polarization, this peak occurred at 3332 cm^{-1}, but not as the main peak. These peaks were placed almost in the wavenumber region for the 3-OH···O-5 intramolecular hydrogen bond that were assigned to the band region of between 3340 and 3375 cm^{-1}.[4,23,24] Wiley and Atalla[22] found a distinct signal at 3334 cm^{-1} in the Raman spectra of Valonia and ramie cellulose, which was the most intense in the 0° polarization mode, and assigned it to have derived from OH stretching vibrations. The peak at 3267 cm^{-1} in the 90° polarization experiment was close to the cellulose Iβ band at 3270 cm^{-1} that was assigned by Sugiyama et al.,[12] which belongs to the wavenumber region of intermolecular hydrogen bonds. The small in-phase signal at 3232 cm^{-1} lies in the suggested wavenumber area for the 6-OH···O-3 intermolecular hydrogen bond between 3230 and 3310 cm^{-1}.[4,8,12,24]

Several overlapping bands appeared between 3000 and 2850 cm^{-1} in both experiments with the main maximum being at 2870 cm^{-1} for 0° polarization, a region typical for CH and CH_2 stretching vibrations.[1,4] However, in 90° polarization, there was one maximum at 2831 cm^{-1} and another overlapping area with peaks at about 2970, 2940, and 2920 cm^{-1}.

In Fig. 3, the difference spectrum of the static absorbance spectra for an oriented sheet is shown (0–90° IR polarizations in relation to fiber direction), which were recorded while the samples were not stretched. Thus, this spectrum indicates which vibrations are oriented in the direction of the cellulose backbone (positive peaks), and which are oriented orthogonal to the backbone (negative peaks). Obviously, the largest peak at 1157 cm^{-1} was a skeletal vibration including the C–O–C

bridge stretching parallel to the backbone. Also, the C–O valence vibration at 1072 cm^{-1} showed a strong orientation effect along the chain. A positive peak also appeared at 1423 cm^{-1}, indicating an orientation along the backbone, which would point to its originating from HOC bending vibrations,[19] rather than CH$_2$ bending earlier suggested.[20] The negative peak at 1458 cm^{-1}, showing an orthogonal orientation, is probably associated to the one at 1462 cm^{-1} in the 90° polarization experiment of Fig. 2. The orthogonal orientation of the vibration in relation to the backbone supports the earlier suggested assignment of the band as a CH$_2$ bending vibration.[1,21] Of the other positive peaks occurring between 1400 and 1200 cm^{-1}, it was mainly the 1369 cm^{-1} band that occurred in the 90° polarization experiments.

For the high wavenumber region of CH and CH$_2$ stretching vibrations, there was a clear negative peak at 2893 cm^{-1}, thus indicating an orthogonal orientation. Interestingly, there were no orientational effects whatsoever for the OH–O hydrogen vibration region of 3200–3500 cm^{-1}. This might be a result of having dipole-moment transition components in both the orthogonal and the parallel directions to the fiber axis.

In Fig. 4, the synchronous 2D spectrum of experiment (A) from Fig. 1 is shown. The correlation spectrum shown is in fact three-di-mensional, with independent wavenumbers on the x- and y-axis and correlation intensities on the z-axis. The advantage of 2D-IR spectra is that they provide simplification of the dynamic spectra (which consist of overlapping peaks) in enhancing the spectral resolution by spreading peaks over a second dimension. Two-dimensional spectra provide information about the interaction between the submolecular groups in relation to the external perturbation, i.e., the sinusoidal strain. In the synchronous spectrum, which is shown, peaks appeared for pairs of bands with similar dynamic behavior. Since the intensity change of each band is obviously correlated with itself, a series of positive maxima along the diagonal (autopeaks) show up. These peaks indicate which transition dipoles, and consequently which functional groups, change dynamically as a result of the applied sinusoidal strain.

In the synchronous correlation spectrum, cross-peaks (off-diagonal-peaks) also appeared, meaning that the corresponding dipole transition moments, which showed up at different wavenumbers, reoriented parallel (positive cross-peak) to each other. For example, a strong cross-peak between the C–O–C asymmetric bridge stretching at 1169 cm^{-1} and the 3-OH···O-5 intramolecular hydrogen bond at 3329 cm^{-1} is marked in Fig. 4. As the response of the measured sample is rather elas-
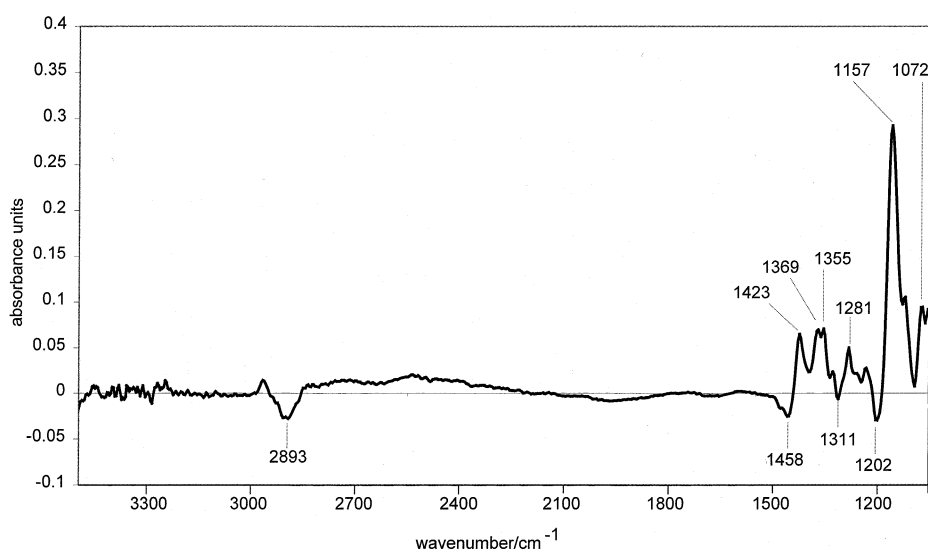

Fig. 3. Difference spectrum of the static absorbance spectra for an oriented sheet (0–90° IR polarization in relation to fiber direction), recorded while the samples were not stretched.
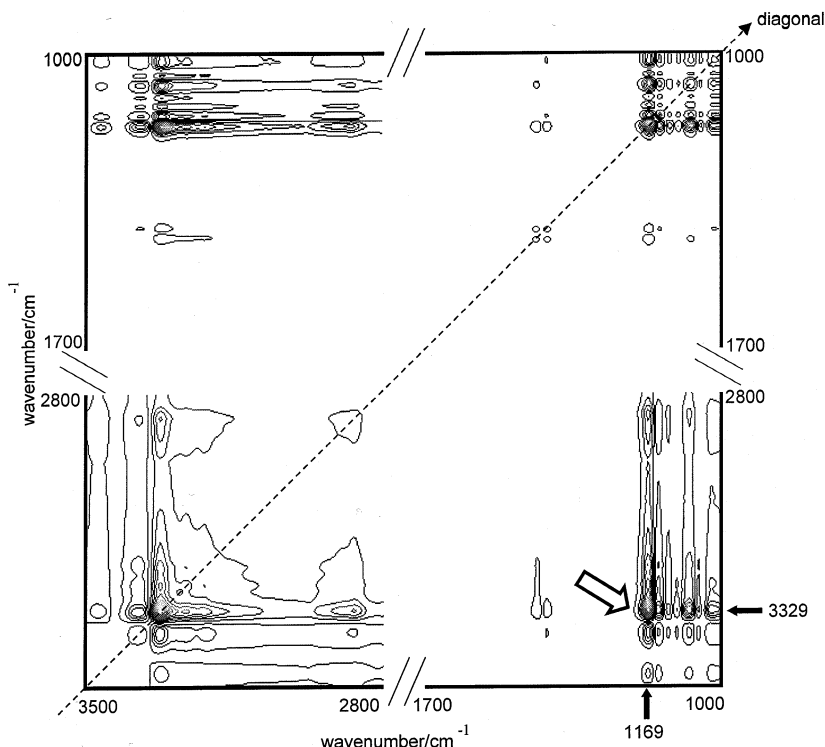
Fig. 4. Synchronous 2D spectrum of experiment (A). The autopeaks are located on the diagonal. The cross-peaks can be seen off the diagonal; one example is marked by an arrow.

tic, cross-peaks can be found between all transition dipoles affected by the applied strain.

In Table 2, all the peaks on the synchronous 2D diagonal for the 0 and 90° polarization experiments are summarized together with assignments according to the literature. It should be noted that most of the literature assignments have been made using the group-frequency approach. Assignments relying on extensive normal coordinate analysis of model compounds such as those of Wiley and Atalla[22] points to most bands below 1400 cm^{-1} representing highly coupled motions that cannot be regarded as local modes.

Effect of fiber direction.—In Fig. 5, the intensities of the peaks on the diagonal, for all experiments with 0° polarization (A, C and E), are shown. The intensity pattern was very similar to that of the in-phase spectrum which, being much more intense than the out-of-phase spectrum, dominated the cross correlation. The bands dominating the diagonal in the 0° polarization mode were 1169 and 3329 cm^{-1} for all the sheets studied. While these two peaks remained at the same wavenumber

for both the differently oriented samples (experiments A and C) and the nonoriented one (experiment E), a difference could be observed in the region between 1100 and 1050 cm^{-1}, which is generally the band region for ring stretching, CC and CO stretching, and CH bending. While there was an intense peak at 1065 cm^{-1} in the perpendicular-oriented sample (experiment C), this peak was smaller, albeit distinct, in the nonoriented sheet (experiment E), and decreased to a small shoulder in the parallel-oriented sheet (experiment A). On the other hand, the small maximum in the parallel-oriented sample at 1076 cm^{-1} (A) became a small shoulder in the nonoriented sheet (E), and was even smaller (relative to the 1065 cm^{-1}) in the perpendicular-oriented sample (C). The 1057 cm^{-1} could only be observed as a real maximum in the nonoriented sample (E).

In the 90° polarization experiments (B, D and F), it was obvious that the dominating peak occurred at 1065 cm^{-1} for all the different cellulose fiber orientations (Fig. 6). It was the most intense for the parallel-oriented and the least intense for the perpendicular-oriented

Table 2
Band assignments of the peaks appearing on the diagonal of the synchronous 2D spectrum, according to the literature

| Wavenumber (cm^{-1}) 2D plot diagonal: 0° polarization	Wavenumber (cm^{-1}) 2D plot diagonal: 90° polarization	Assignment	Literature (Ref. no.)
3329	3332	3340–3375 3-OH···O-5 intramolecular H-bond	4,24
3275	3267	3270 cellulose I β, 3230–3310 6-OH···O-3 intermolecular H-bond	4,8,12,24
	(3232)	3240 cellulose I α	12
2943, 2893, 2874	several small between 2840–2943	2980–2835 sym and asym CH$_2$ stretching vibration, CH stretching vibration	1,4,21,24
	1462	1460 CH$_2$ sym bending in 90° polarization	1,21
1435	1435	CH$_2$ scissor motion, 1430–1500 HCH bending	20,22
	1373	CH bending, COH bending	11,20,21,22
	1319	1315–1335 CH$_2$ wagging in 90° polarization	20,21
1169	1165	C–O–C asym bridge stretching, 950–1180 CC and CO stretching	20,21,22
1150		C–O–C asym valence vibration, CC and CO stretching vibration and CH bending, 950–1180 CC and CO stretching	1,11,22
1126	1126	1125–1162 C–O–C asym valence vibration, 950–1180 CC and CO stretching	11,22
	1115	1115–1120 ring stretch, CC and CO stretching	1,11,20,22
(1076)	(1076)	1075 CC and CO stretching, CH bending	1
1065	1065	1015–1060 C–O valence vibr.	11
1057		1015–1060 C–O valence vibr.	11
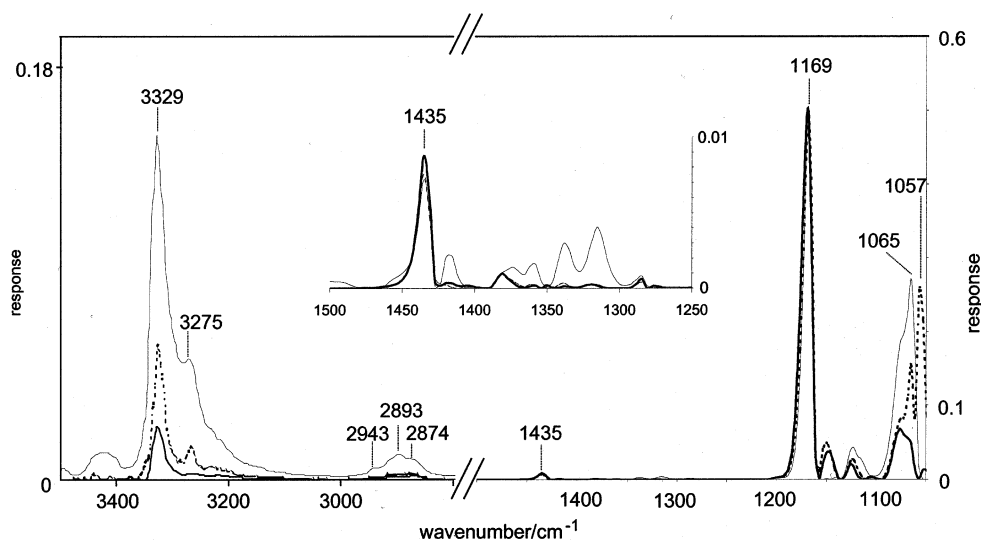
Fig. 5. Diagonals of the synchronous 2D plot of the IR responses during 0° polarization showing the result of the sheet stretched parallel to the fiber axis (thick solid line), perpendicular to the fiber axis (thin solid line), and a nonoriented sheet (dotted line).

Fig. 6. Diagonals of the synchronous 2D plot of the IRresponses during 90° polarization showing the result of the sheet stretched parallel to the fiber axis (thick solid line), perpendicular to the fiber axis (thin solid line), and a nonoriented sheet (dotted line).
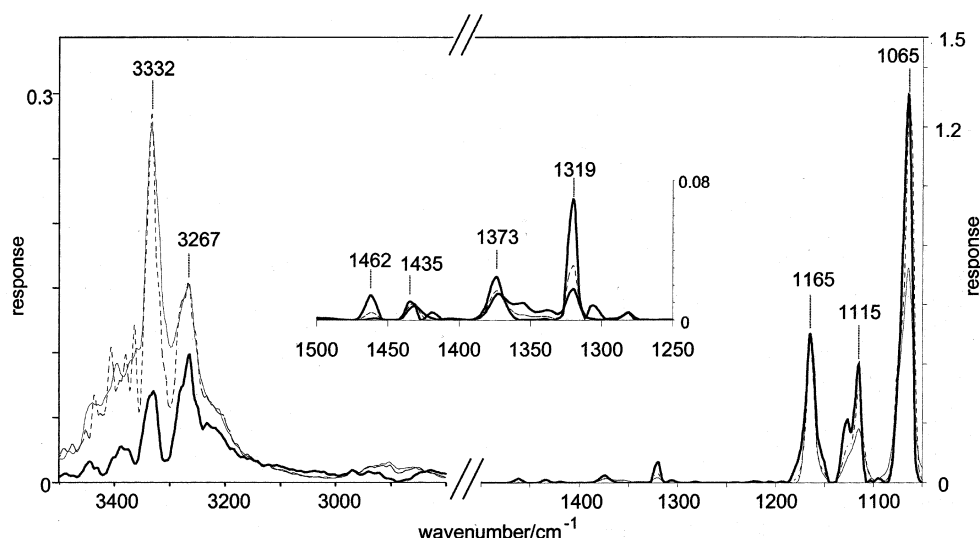
sheets, while the intensity for the nonoriented sample lay in-between. For the perpendicular and the nonoriented sheets, a shoulder at 1076 cm^{-1} could also be recognized.

With regard to the higher wavenumbers, the peaks at 1169 and 1165 cm^{-1} corresponding to the 0 and 90° polarization modes, respectively, were both recognized as very sharp bands. While the 1169 cm^{-1} was the most intense peak in the 0° polarization experiment, this vibration occurred as the 1165 cm^{-1} band, being one among others, in the 90° experiment.

When comparing the results shown in Figs. 5 and 6, it was also obvious that the peak at 1435 cm^{-1} appeared in all the experiments, being more intense within the 0° polarization mode than within the 90° polarization mode. On the other hand, the peaks that appeared between 1120 and 1115 cm^{-1} (ring-stretching and CO stretching bands according to Atalla[3]) were more intense in the 90° polarization mode than in the 0° polarization mode. Only small, broad peaks arose in the 0° experiment, the most intense being for the perpendicular orientation followed by the nonoriented and the parallel-oriented samples. For the 90° polarization experiment, the peaks were most intense (showing nice distinct bands) for the parallel-oriented sheets, followed by the nonoriented and the perpendicular-oriented samples. The same effect was evident for the small peak at 1319 cm^{-1}.

For the OH region in 0° polarization (Fig. 5), the 3329 cm^{-1} peak was the most intense in the perpendicular-oriented sample (C), less so in the nonoriented sheet (E), and even smaller in the parallel-oriented sample (A).

In Fig. 6 (the 90° polarization mode), it is most noticeable that more signals appeared in the OH-region than that in 0° polarization, the main one being at 3332 cm^{-1} for the nonoriented and perpendicular-oriented sheets. For the parallel-oriented sheet, the main peak was at 3267 cm^{-1} representing vibrations of intermolecular hydrogen bonds.[4,8,12,24]

In general, in both the 0 and 90° polarization modes, whenever comparing band shapes or intensities from the spectrum of parallel-orientation with perpendicular-orientation, the spectra of the nonoriented would lie in between the spectra of these two directions.

4. Discussion

Several peaks appeared in the in-phase spectra and the 2D plot diagonals, derived mainly from the skeletal vibrations including the C–O–C bridge connecting adjacent glucose rings, and the signals from the hydrogen bonds. There were hardly any signals derived from CH vibrations. This supported the calculations of Tashiro and Kobayashi,[1] who found that the strain energy distribution goes mainly

via the glucose rings ($\sim$30%), the C–O–C bridge ($\sim$20%), and the 3-OH⋯O-5 intramolecular hydrogen bond ($\sim$20%), while the distribution via the 2-OH⋯O-6 intramolecular hydrogen bond is negligibly small.

The peak for the skeletal C–O–C vibration is generally expected to be at about 1160 cm^{-1}, which was found in the static spectra of all the samples in this study, as well as the differential spectrum shown in Fig. 3. The shift to a higher wavenumber in the dynamic spectra (peak position at 1169 cm^{-1} for the 0° polarization mode), and therefore higher energy, was probably a result of the stretching of the cellulose molecules oriented in the stretching direction. This stretching affects the ether linkage by changing the angle between the C and the O, and the C of the following ring, and therefore changing the energy. Such a shift in energy is also compatible with the peak splitting, as seen by the in-phase spectra of Fig. 1. For both the 0 and 90° polarization modes, there seems to be a strong relation between the skeletal vibration/C–O–C band at 1169 cm^{-1} and the peak at 1435 cm^{-1}, as the normalization at the 1169 cm^{-1} band resulted in an independence from sheet orientation at 1435 cm^{-1}. This is a good indication that the 1435 cm^{-1} peak derives from HOC bending rather than CH$_2$ scissors motion. Furthermore, the 1435 cm^{-1} band was split like the 1169 cm^{-1} band. Due to the Poisson effect, the sheet should also experience a deformation perpendicular to the stretching direction. Thus, the peak at 1165 cm^{-1} for the 90° polarization mode was highly expected, while at the same time not surprising that it was not the dominating peak.

As the peak at 1462 cm^{-1} represents an orthogonal vibration in relation to the backbone, its appearance in the 90° polarization experiment was also not surprising since it derived from the stretching of the cellulose chains in the direction of the stretch.

As the hydrogen-bonding region was not showing any orientation dependence, its relation to the C–O–C stretching or skeletal vibrations in terms of the different sheets would not be expected to be so strong. The high intensity for the 3-OH⋯O-5 intramolecular hydrogen vibration, 3329/3332 cm^{-1}, is clearly pointing to its importance in the loading of the cellulose chain. The fact that it is highest in both the 90 and 0° polarization modes for the sheet loaded perpendicular to the fiber axis, and least for the sheet loaded parallel to the fiber axis, is related to the normalization at 1165 and 1169 cm^{-1}, respectively. In the perpendicularly oriented case, of the cellulose chains capable of taking up load, few are oriented more or less in the stretching direction, resulting in a low dynamic intensity of the C–O–C stretching vibration. Thus, in this case, the overall deformation by bending and shearing of the fibers would show up as a larger change in the 3-OH⋯O-5 intramolecular hydrogen bond deformation.

In all cases the most intense peak of the hydrogen-bonding region was at 3329/3332 cm^{-1} (intramolecular hydrogen bond) except for the sheet stretched parallel to the fiber axis and examined at 90° polarization where the intermolecular hydrogen bond at 3267 cm^{-1} was the most intense (Figs. 5 and 6). These intermolecular hydrogen bonds build up the sheet structure of cellulose and are responsible for the high modulus in the sheet planes perpendicular to the chain axis.[1] The straining of the oriented sheet parallel to the fiber orientation, due to the Poisson effect, will result in an appreciable deformation perpendicular to the fiber orientation. Thus, when in this case examining the resulting molecular changes in 90° polarization, it is not surprising that the intermolecular ones dominate over the intramolecular hydrogen bonds.

5. Conclusions

Cellulose fibers showed a mainly elastic response when stretched periodically with a small amplitude. The dynamic FTIR analysis indicated that, on the molecular level, the strain distribution goes via the glucose ring, the C–O–C linkage between these rings, and the 3-OH⋯O-5 intramolecular hydrogen bond, whereas the 2-OH⋯O-6 intramolecular hydrogen bond seems to play a minor role. The intermolecular hydrogen bonds are shown to be more affected by deformation perpendicular to the fiber axis. Furthermore, the results showed that for cellulose in a fiber network

material like paper, the fiber direction towards the stretching direction is not of main importance in experimental arrangements for dynamic FTIR studies, since the same peaks for the cellulose appeared for all fiber directions examined. Small shifts in wavenumber could be due to anisotropy effects. The main effect observed for the different fiber directions was the differences in intensity proportions. The direction of the incident polarized IR beam towards the stretching direction was therefore found to be of the main interest in evaluating dynamic FTIR spectra.

Acknowledgements

References

1. Tashiro, K.; Kobayashi, M. *Polymer* **1991**, *32*, 1516–1526.

2. O'Sullivan, A. C. *Cellulose* **1997**, *4*, 173–207.
3. Atalla, R. H. In *Comprehensive Natural Products Chemistry*; Barton, D.; Nakanishi, K.; Meth-Cohn, O., Eds. Celluloses, first edition; Elsevier Science: Oxford, 1999; Vol. 3, pp. 529–598.
4. Liang, C. Y.; Marchessault, R. H. *J. Polym. Sci.* **1959**, *37*, 385–395.
5. Atalla, R. H. *Science* **1984**, *223*, 283–285.
6. Cael, J. J.; Gardner, K. H.; Koenig, J. L.; Blackwell, J. *J. Chem. Phys.* **1975**, *62*, 1145–1153.
7. Mann, J.; Marrinan, H. J. *J. Chem. Soc., Faraday Trans. 1*, **1956**, 492–497.
8. Siesler, H.; Krässig, H.; Grass, F.; Kratzl, K.; Derkosch, J. *Angew. Makromol. Chem.* **1975**, *42*, 139–165.
9. Nishiyama, Y.; Isogai, A.; Okano, T.; Müller, M.; Chanzy, H. *Macromolecules* **1999**, *32*, 2078–2081.
10. Michell, A. J. *Carbohydr. Res.* **1990**, *197*, 53–60.
11. Fengel, D.; Ludwig, M. *Papier* **1991**, *45*, 45–51.
12. Sugiyama, J.; Persson, J.; Chanzy, H. *Macromolecules* **1991**, *24*, 2461–2466.
13. Noda, I.; Dowrey, A. E.; Marcott, C. *Mikrochim. Acta (Wien)* **1988**, *1*, 101–103.
14. Palmer, R. A.; Manning, C. J.; Chao, J. L.; Noda, I.; Dowrey, A. E.; Marcott, C. *Appl. Spectrosc.* **1991**, *45*, 12–17.
15. Noda, I. *J. Am. Chem. Soc.* **1989**, *111*, 8116–8118.
16. Hinterstoisser, B.; Salmén, L. *Cellulose* **1999**, *6*, 251–263.
17. Hinterstoisser, B.; Salmén, L. *Vib. Spectrosc.* **2000**, *22*, 111–118.
18. Manning, C. *Polymer Modulator;* Troy, ID, USA: Manning Applied Technologies Inc., 1997.
19. Atalla, R. H. personal communication, 2001.
20. Liang, C. Y.; Marchessault, R. H. *J. Polym. Sci.* **1959**, *39*, 269–278.
21. Marchessault, R. H. *Pure Appl. Chem.* **1962**, *5*, 107–129.
22. Wiley, J. H.; Atalla, R. H. *Carbohydr. Res.* **1987**, *160*, 113–119.
23. Fengel, D. *Holzforschung* **1993**, *47*, 103–108.
24. Ivanova, N. V.; Korolenko, E. A.; Korolik, E. V.; Zhbankov, R. G. *Zh. Prikl. Spektrosk.* **1989**, *51*, 301–306.